Physical and Photophysical Characterization of a BODIPY Phosphatidylcholine as a Membrane Probe

Mohammed Dahim, Nancy K. Mizuno, Xin-Min Li, William E. Momsen, Maureen M. Momsen, and Howard L. Brockman

The Hormel Institute, University of Minnesota, Austin, Minnesota 55912 USA

ABSTRACT   Lipids containing the dimethyl BODIPY fluorophore are used in cell biology because their fluorescence properties change with fluorophore concentration (C.-S. Chen, O. C. Martin, and R. E. Pagano. 1997. *Biophys J.* 72:37–50). The miscibility and steady-state fluorescence behavior of one such lipid, 1-palmitoyl-2-(4,4-difluoro-5,7-dimethyl-4-bora-3a,4a-diaza-*s*-indacene-3-pentanoyl)-*sn*-glycero-3-phosphocholine (PBPC), have been characterized in mixtures with 1-stearoyl-2-oleoyl-*sn*-glycero-3-phosphocholine (SOPC). PBPC packs similarly to phosphatidylcholines having a *cis*-unsaturated acyl chain and mixes nearly ideally with SOPC, apparently without fluorophore–fluorophore aggregation. Increasing PBPC mole fraction from 0.0 to 1.0 in SOPC membranes changes the emission characteristics of the probe in a continuous manner. Analysis of these changes shows that emission from the excited dimethyl BODIPY monomer self quenches with a critical radius of 25.9 Å. Fluorophores sufficiently close (≤13.7 Å) at the time of excitation can form an excited dimer, emission from which depends strongly on total lipid packing density. Overall, the data show that PBPC is a reasonable physical substitute for other phosphatidylcholines in fluid membranes. Knowledge of PBPC fluorescence in lipid monolayers has been exploited to determine the two-dimensional concentration of SOPC in unilamellar, bilayer membranes.

INTRODUCTION

To minimize membrane perturbation, an acyl fluorophore-containing lipid analog should resemble as closely as possible the species it replaces, particularly with respect to polarity and cross-sectional area in the membrane. Any membrane perturbation inherent in using a lipid analog can be further exacerbated if the application requires the probe to be present in more than trace mole fractions relative to total lipid. For example, as their membrane abundance is increased, lipid acyl groups labeled with planar polycyclic fluorophores, like anthracene (Rodriguez et al., 1995), diphenylhexatriene (DPH) (Lentz and Burgess, 1989) and even the widely used pyrene (Lemmetyinen et al., 1989; Merkel and Sackmann, 1994), tend to form aggregates. Like probe size and polarity, aggregation can perturb membrane structure and compromise probe usefulness.

A recently developed family of fluorophores is based on the relatively compact 4,4-difluoro-4-bora-3a,4a-diaza-*s*-indacene moiety, called BODIPY (Johnson et al., 1991). BODIPY derivatives are more hydrophobic than the commonly used 7-nitro-2,1,3-benzoxadiazol-4-yl (NBD) group, but less hydrophobic than pyrene (Kaiser and London, 1998). Unlike pyrene or NBD, the fluorescence emission of BODIPY chromophores is relatively insensitive to environmental factors like medium polarity, pH, and oxygen (Johnson et al., 1991; Karolin et al., 1994) as well as membrane potential (Pagano et al., 1999). BODIPY fluorescence decays monoexponentially in membranes (Karolin et al.,

1994) with a relatively short lifetime of 5–6 ns. Because of these desirable properties, BODIPY fluorophores have found wide application for studying the solution structure of proteins (Bergström et al., 1999), for assaying enzymes and for imaging (Farber et al., 2001). BODIPY fluorophores are generally nontoxic to cells (Wories et al., 1985) and can be used to study lipid metabolism (Kasurinen, 1992), lipid transport (Pagano et al., 1999), and to diagnose diseases (Chen et al., 1999).

Like pyrene, two molecules of the dimethyl BODIPY fluorophore can form an excited-state dimer, termed an excimer, that exhibits a second emission peak red-shifted from that arising from the excited monomer. This dependence of excimer emission on fluorophore abundance has been used to show that the mole fraction of exogenously added lipids containing the BODIPY fluorophore can become as high as 0.10 in endosomes (Chen et al., 1997) and provides the basis of a clinical diagnostic technique (Chen et al., 1999). The application assumes explicitly that the emission properties of the fluorophore are identical in cells and model phospholipid vesicles used for calibration, and, implicitly, that probe emission properties in cells are independent of total lipid packing density (Pagano et al., 1999). In part, these assumptions have remained untested because lipid packing density itself in fluid model bilayer membranes is difficult to measure, even when only a single lipid species is present (Costigan et al., 2000). The utility of dimethyl BODIPY lipids to assess the abundance of particular lipid species as they move within cells and, more generally, to serve as quantitative fluorescent reporters of membrane lipid composition shows the need for a better understanding of how these lipids pack in membranes and how that regulates their fluorescence emission.

As a first step, this paper describes the physical and photophysical properties of a dimethyl BODIPY-containing phospholipid, 1-palmitoyl-2-(4,4-difluoro-5,7-dimethyl-4-bora-3a,4a-diaza-*s*-indacene-3-pentanoyl)-*sn*-glycero-3-phosphocholine (PBPC) in lipid monolayers at the gas–liquid interface. Monolayers offer particular advantages for this characterization over other model membrane systems. Specifically, with monomolecular films, exciton migration is confined to a single plane, thereby avoiding the complexities of interpretation caused by transbilayer interactions of fluorophores (Baumann and Fayer, 1986). Light scattering artifacts associated with bilayers (Ladokhin et al., 2000) are also eliminated. Last, at any given lipid composition, the lipid and, hence, fluorophore concentration, is known and can be systematically varied over greater than a twofold range. In contrast, the range of area changes available from thermal expansion of bilayers is typically only 2.3×10^{-3} K^{-1} (Galla et al., 1979). The results show that PBPC packs comparably to other typical phosphatidylcholines containing acyl chain unsaturation and mixes nearly ideally with 1-stearoyl-2-oleoyl-*sn*-glycero-3-phosphocholine (SOPC). Monomer and excimer fluorescence emission intensities of PBPC in monolayers are controlled by PBPC composition, PBPC concentration, and total lipid-packing density. With knowledge of the emission properties of PBPC in monolayers, the packing density of SOPC in unilamellar bilayers has been measured.

MATERIALS AND METHODS

Reagents

PBPC was from Molecular Probes (Eugene, OR). SOPC, 1-stearoyl-2-azrachidonyl-*sn*-glycero-3-phosphocholine (SAPC), and 1,2-diarachidonoyl-*sn*-glycero-3-phosphocholine (DAPC) were from Avanti Polar Lipids (Alabaster, AL). The purification of water and preparation of solvents, buffer, and lipid solutions have been previously reported (Momsen et al., 1997).

Methods

As received from the manufacturer, PBPC exhibited surface pressure–molecular area isotherms that were inordinately large and irreproducible from lot to lot. Accordingly, it was chromatographically purified by isocratic HPLC on a Beckman 344 liquid chromatograph using a Brownlee Spheri-5 silica 100 × 4.6 mm column preceded by a Newguard silica 15 × 3.2 mm cartridge (Alltech Associates, Inc., Deerfield, IL). The column was pre-equilibrated with 30 ml chloroform/methanol/water (60:40:4) at a flow rate of 2 ml/min. An aliquot of ~0.8 μmole PBPC (~8.3 μmole/ml) in the same solvent was applied to the column, and PBPC was eluted with 11 ml of the equilibration solvent. The column was washed with 9 ml methanol at 1 ml/min, after which the equilibration and elution procedure was repeated with the next aliquot. Elution of the highly fluorescent PBPC was monitored visually using long-wave UV (365 nm) excitation, and 3–4 fractions were collected manually. Peak fractions from several aliquots were combined, and the resulting sample was concentrated and repurified in 0.8-μmole aliquots using the same protocol. The final product was dried under N_2 and redissolved in benzene. Purified PBPC exhibited an extinction coefficient in ethanol at 505 nm of 84,400 $cm^{-1}M^{-1}$ using as a

reference a PBPC solution that had been calibrated by assaying lipid phosphorous (Bartlett, 1959).

The automated, Langmuir-type film balance used for obtaining surface pressure–dipole potential–lipid concentration isotherms has been recently described (Li et al., 2001). Isotherms were collected at 24°C under a humidified argon atmosphere on an aqueous subphase of phosphate-buffered saline (10 mM potassium phosphate, pH 6.6, 0.1 M NaCl, 0.01% NaN_3). PBPC was spread from benzene and the other lipids from hexane/ethanol (95:5). The film was compressed at a rate ≤0.25 molecule min/Å^2 to beyond its collapse pressure. Surface pressure–lipid concentration isotherms for fluorescence and optical absorption studies were collected using a Kibron Micro Trough (Kibron, Inc., Helsinki, Finland). Temperature was maintained at 24°C using a home-built circulating plate attached to a thermostated circulating water bath. The working area of the glass/Teflon trough was 115 cm². To form monolayers at the air–buffer interface at a selected initial lipid concentration, mixtures of lipids in benzene, typically 7–11 μl, were spread onto a cleaned aqueous subphase of phosphate-buffered saline. After waiting 5 min for the solvent to evaporate, the lipid monolayer was symmetrically compressed to the desired final concentration at a rate of 0.4 molecule min/Å^2. Longer waiting times made no measurable difference in the isotherms obtained. With this small trough, reproducibility of lipid concentration measurements at 20 mN/m for replicate isotherms was ±5%.

For the simultaneous recording of fluorescence with monolayer compression, the base plate of the Kibron film balance was fitted with home-built attachments for fiber optic cables and collimators. An opaque, blackened box having a port for surface cleaning and sample addition covered the entire trough assembly. Incident light at 488 nm was provided by a model 2122-45L argon-ion laser (JDS Uniphase, San Jose, CA) equipped with a model 3 light-intensity controller and a fiber optic coupler model HPUC-23-488-S-3, FAC-2BL (Oz Optics, Nepean, ON, Canada). After exiting a collimator, the light passed through a 2° holographic diffusing filter (Coherent, Auburn, CA) and was masked to project a circular spot of ~0.5-cm diameter on the monolayer surface. The angle of incidence of the unpolarized light beam with respect to the monolayer surface was ~30° and the measured intensity in the projected spot was ~1.5 mW/cm². Fluorescence emission was collected perpendicular to the interface at a distance of ~1 cm using an Ocean Optics model PC2000-ISA fiber optic spectrometer equipped with an L2 lens and 200-μm slit (Ocean Optics, Dunedin, FL). For experiments to study monolayer–bilayer equivalence, the diffusing filter was omitted from the excitation path, and a 500-nm-long pass filter (500EFLP, Omega Optical, Brattleboro, VT) was mounted between the emission collimator and the detector to reduce scattered excitation light. Fluorescence emission spectra and emission intensities averaged over particular wavelength windows were collected each second, and an average of 10 such readings was recorded every 10 s using the manufacturer's OOIBase32 software. The window for averaging monomer emission from PBPC was defined as the average of intensities from 510 to 520 nm and excimer emission as the average from 600 to 620 nm. Although monolayer compression was continuous during the spectral data-acquisition cycle, the fractional change in lipid concentration during each acquisition cycle was ≤0.0073. Control experiments showed that emission spectra were independent of the gas phase, i.e., air or argon, and of the presence or absence of 0.01% sodium azide preservative in the subphase buffer. At each collection of emission-intensity data, the entire emission spectrum was also collected and stored separately. Each isotherm reported is an average of at least two determinations to correct for small changes in the fiber-optical path that occurred when the cover was removed between runs.

Optical absorbance was recorded during monolayer compression in a manner similar to that described above. A 1″-diameter collimator/focusing lens assembly (#77330, Thermo Oriel, Atlanta, GA) was mounted above a Kibron trough in the same manner as the collimator used for fluorescence measurements. The collimator was illuminated through the lipid monolayer from below by a white LED (#606-CMD333VWC, Mauser Electronics, Mansfield, TX). The light entering the collimator/focusing assembly was

carried by a fiber-optic cable to a spectrograph (MS127*i*, Thermo Oriel) to which was mounted a thermoelectrically cooled CCD array detector (Model DV420-BU2, Andor Technology, South Windsor, CT). Absorbance spectra were accumulated for 10 s before being recorded, and, for presentation, were baseline corrected using data obtained at wavelengths $>$ 550 nm.

Large unilamellar vesicles were prepared using established procedures (MacDonald et al., 1991). Lipid, 25 nmol of SOPC or an SOPC-PBPC mixture, was dried for at least 2 hr under high vacuum. To this was added 1 ml phosphate-buffered saline, and the sample was vortexed for 60 s. It was then freeze–thawed 10 times using an isopropanol-dry ice mixture, extruded 15 times through 100-nm Nucleopore filters (Costar Scientific Corp, Cambridge, MA), placed in a cylindrical glass cuvette (32-G-10, Starna Cells, Atascadero, CA) and made up to a volume of 3.4 ml. Fluorescence emission spectra of the bilayer vesicles were measured with essentially the same apparatus as used for the monolayer measurements. Instead of the glass Kibron trough, the cylindrical cuvette was positioned on the Kibron base plate under the detection collimator so that light from the laser entered the curved side of the cuvette while one flat face of the cuvette faced the detector. The reference spectrum for bilayer fluorescence measurements was a sample of SOPC vesicles. The spectrum of these unlabeled vesicles was indistinguishable from that obtained with buffer alone, demonstrating the absence of a significant contribution of scattered light to the measured fluorescence.

Analysis of surface pressure–dipole potential–concentration isotherms

Collapse pressures of surface pressure–concentration isotherms of pure lipids and mixtures were identified using a combination of second and third derivatives of surface pressure with respect to the reciprocal of total lipid concentration, i.e., molecular area, A, as previously described (Brockman et al., 1980). Monolayer collapse areas were calculated by extrapolation of fitted surface pressure–molecular area isotherms (below) to the collapse surface pressure. The collapse pressures of mixed monolayers were calculated as described by Joos (1969) using the mixture compositions and the collapse surface pressures of the pure components. The Joos formalism assumes that the mixing of the lipids in the monolayer is thermodynamically ideal. Ideal molecular area, A_I, for lipid mixtures was defined by the additivity rule (Gaines, 1966),

$$A_I = \sum (A_i X_i), \tag{1}$$

where A_i is the partial molecular area of the *i*th lipid species at π, and X_i is its mole fraction. Using this relationship, ideal surface pressure–molecular area isotherms at desired compositions were generated over a range of surface pressures using the isotherms of the pure lipids.

Surface pressure–molecular area isotherms of pure lipids were analyzed using an osmotic-based equation of state (Feng et al., 1994),

$$\pi = (qkT/A_1)\ln[(1/f_1)[1 + A_1/(A - A_\infty)]]. \tag{2}$$

The cross-sectional area of a water molecule, A_1, is taken as 9.65 Å^2, k is the Boltzmann constant and T is the absolute temperature. The fitting parameter, A_∞, is the lipid molecular area extrapolated to infinite pressure. In the context of the model, it is essentially the cross-sectional area of the totally dehydrated lipid molecule in the plane of the interface. The fitting parameters f_1 and q, which describe isotherm shape, are related (Smaby and Brockman, 1991) and only values of f_1 are reported. The parameter f_1 is the activity coefficient of water at the liftoff area of the monolayer.

The surface pressure–molecular area isotherms of ideal and experimental lipid mixtures were analyzed using Eq. 2 adapted to mixtures (Smaby and Brockman, 1992) for which

$$A_\infty = \sum (A_{\infty,i} X_i) \quad q = f(q_i, X_i) \quad f_1 = f(f_{1,i}, X_i).$$

As previously described, experimental data for pure lipids and mixtures fit to Eq. 2 were analyzed between a surface pressure of 1 mN/m and the molecular area at which $d^2\pi/dA^2$ goes from positive to negative (Smaby and Brockman, 1990). The same range was then used for the ideal isotherm for lipid mixtures to obtain the ideal values of the parameters, $A_{\infty,I}$, q_I, and $f_{1,I}$. If satisfactory fits of experimental and ideal π-A isotherms for mixtures are obtained using Eq. 2, the values of the fitting parameters can be compared to characterize the miscibility behavior of the lipids (Smaby and Brockman, 1992).

The compressibility of a lipid monolayer is $C_s = (-1/A)(dA/d\pi)$. To follow the convention in the literature, values of compressibilities are expressed as their reciprocals, C_s^{-1}, the modulus of compression. The ideal modulus of the mixed monolayer at a surface pressure, π, is calculated from the compressibilities of the pure lipids by (Ali et al., 1994),

$$C_{s,I}^{-1} = -A_I/\sum(C_{s,i}A_iX_i). \tag{3}$$

Dipole potential, ΔV, isotherms of single-component lipid monolayers were analyzed according to the linear relationship (Smaby and Brockman, 1990),

$$\Delta V = \Delta V_0 + 37.70 \ \mu_\perp/A, \tag{4}$$

where ΔV_0 is a constant related to the effect of the lipid headgroup on the structure of interfacial water relative to a lipid-free interface (Brockman, 1994) and $\mu_\perp$ is the component of the dipole moment perpendicular to the interface. For ideal mixed lipid monolayers, it has been shown that (Smaby and Brockman, 1992),

$$\Delta V_{0,I} = \sum(\Delta V_{0,i}A_iX_i/A_I) \quad \text{and} \quad \mu_{\perp,I} = \sum(\mu_{\perp,i}X_i).$$

These definitions and the ideal π-A_I isotherms determined as described above allow ideal values of $\Delta V_{0,I}$ and $\mu_{\perp,I}$ to be calculated for any ideal mixture if the corresponding parameters for the pure lipids constituting the mixture are known (Smaby and Brockman, 1992). If experimental plots of ΔV versus $1/A$ for mixtures are also linear, then the values of ΔV_0 and $\mu_\perp$ obtained from them using Eq. 4 can be compared to the ideal values to help characterize the miscibility of the lipids.

Monolayer collapse pressures, collapse areas, moduli of compression, π-A-ΔV isotherm fitting parameters and the wavelengths of spectral maxima were determined using FilmFit software (Creative Tension, Austin, MN). Fitting to determine the model parameters describing monomer and excimer emission intensity was performed using the nonlinear least squares capability of Origin 6.0 (OriginLab Corp, Northhampton, MA).

RESULTS

Physical behavior of PBPC in monolayers

To characterize the packing properties of the fluorophore-containing phosphatidylcholine, PBPC, relative to other diacyl phosphatidylcholine species, surface pressure–dipole potential–lipid concentration isotherms were measured at 24°C (Fig. 1). Each surface pressure–concentration isotherm shown is an average of three or more isotherms for each lipid. In addition to pure PBPC (Fig. 1, *diamonds*) the other pure lipid species characterized were SOPC (*dotted line*), SAPC (*dashed line*) and DAPC (*dash-dot line*).
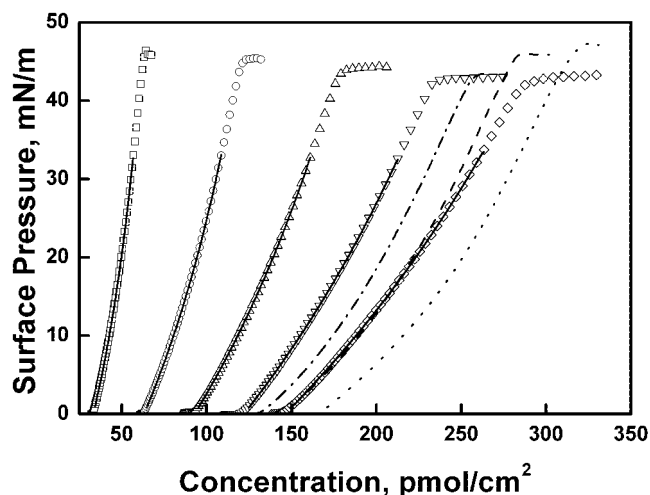
FIGURE 1 Surface pressure–concentration isotherms for PBPC and other diacyl phosphatidylcholines at the argon–buffer interface. Each data set is the average of three or more isotherms obtained at 24°C and only every third data point is shown. SOPC (- - - -); SAPC (– – –); DAPC (– · – ·); PBPC (◇); PBPC:SOPC, 80/20 (▽); PBPC:SOPC, 60/40 (△); PBPC:SOPC, 40/60 ○; PBPC:SOPC, 20/80 (□). Isotherms for PBPC-SOPC mixtures, but not pure lipids, are plotted versus PBPC concentration for clarity. The solid lines for the data sets with symbols were obtained by fitting the data to Eq. 2 over the range indicated by the line.

Shown also are isotherms obtained with mixtures of PBPC and SOPC. These isotherms (*symbols*) are presented as a function of the concentration of PBPC, i.e., the total lipid concentration multiplied by the mole fraction of PBPC in the mixture. This separates the isotherms graphically from those of the pure lipid species and makes the presentation consistent with that used in the fluorescence analysis presented below. In our experience, these phosphatidylcholines, which contain *cis*-unsaturated acyl moieties, exemplify the range of packing behavior exhibited by this lipid class in the liquid-expanded state.

Inspection of the data in Fig. 1 shows that at 24°C pure PBPC (*diamonds*) is in the liquid-expanded phase at all surface pressures below monolayer collapse and falls within the range of the other phosphatidylcholines tested (*lines without symbols*). Up to ~20 mN/m, the surface pressure–concentration isotherm of PBPC is identical to that of SAPC (*dashed line*). As the pressure exceeds 20 mN/m, however, PBPC packs more closely than SAPC and, at its monolayer collapse concentration of 285 pmol/cm^2, its molecular area

TABLE 1 Phosphatidylcholine monolayer parameters

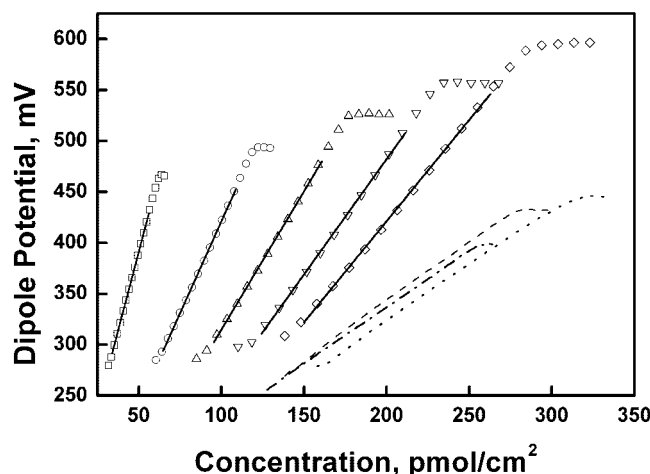| Lipid	$C_{s,25}^{-1}$ (mN/m)	$A_{collapse}$, (Å^2/molec)	$\pi_{collapse}$ (mN/m)	A_∞ (Å^2/molec)	f_1	ΔV_0 (mV)	$\mu_\perp$ (mD)
SOPC	100	53.6	47.2	40.0	1.16	102	488
PBPC	78	58.3	42.4	30.4	1.12	24	874
SAPC	92	59.8	46.0	41.0	1.13	111	511
DAPC	90	65.8	42.9	42.5	1.12	116	487

FIGURE 2 Dipole potential–concentration isotherms for PBPC and other diacyl phosphatidylcholines at the argon–buffer interface. Conditions, lines and symbols are as in Fig. 1. Isotherms for PBPC-SOPC mixtures, but not pure lipids, are plotted versus PBPC concentration for clarity. The solid lines for the data sets with symbols were obtained by fitting the data to Eq. 4 over the range indicated by the line.

is 58.3 Å^2, a value 1.5 Å^2 smaller than for SAPC (Table 1). This shape difference is reflected in the modulus of compression of PBPC being slightly lower, 78 mN/m, at a surface pressure of 25 mN/m compared to 90–100 mN/m for the other expanded phosphatidylcholines (Table 1). The measured collapse surface pressure of PBPC, 42 mN/m, is similar to that of DAPC, but is slightly lower than those of the other phosphatidylcholines (Table 1). An additional comparison of the isotherms for the pure lipids and mixtures can be made by analysis of the shape and size of the liquid-expanded isotherms using an equation of state, Eq. 2. The isotherms for PBPC and its mixtures with SOPC gave excellent fits in all cases (Fig. 1, *solid lines*), as did those for the other pure phosphatidylcholines (fit lines not shown). The characteristic parameters, A_∞ and f_1, for the pure phosphatidylcholines are given in Table 1. The values of f_1 are similar for the lipids. However, the value of the parameter A_∞, that represents the hard cylinder area of the dehydrated lipid, is unusually small for PBPC, compared to the other fluid lipids.

Another characteristic property of membrane lipids is the dipole potential that they and bound water molecules create between bulk water and the hydrocarbon center of the membrane (Brockman, 1994). Dipole potentials, measured during collection of the compression isotherms described above, are shown in Fig. 2. Inspection of the data shows that, as the monolayer of PBPC is compressed (Fig. 2, *diamonds*), its potential rises continuously but more rapidly than those of the other liquid-expanded phosphatidylcholines (*lines without symbols*), reaching ~600 mV at collapse, a value ~150 mV higher than for the other expanded phosphatidylcholines. As described in Materials and Meth-
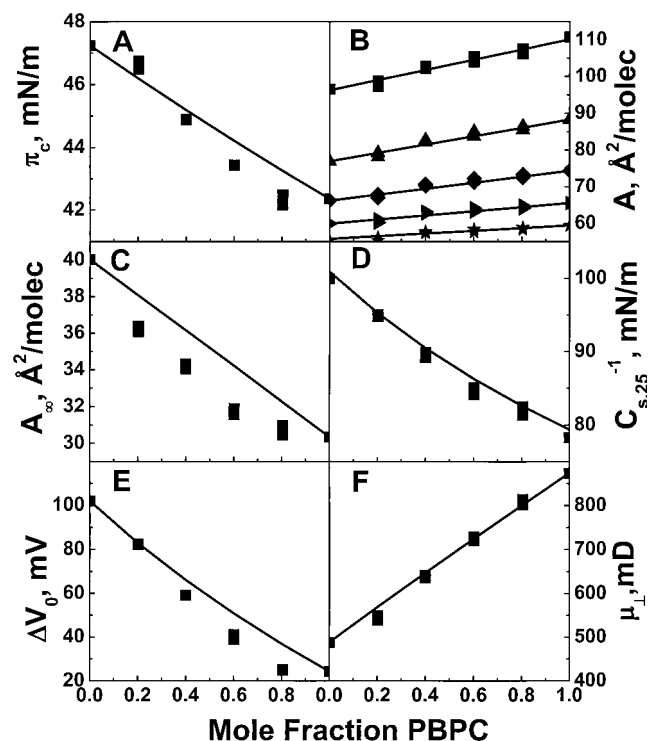
FIGURE 3 Characterization of PBPC-SOPC miscibility. The fitting parameters (*data points*) and ideal curves (*solid lines*) were calculated from the data shown in Figs. 1 and 2 as described in Materials and Methods. *Panel B*, top to bottom, surface pressures are 1, 10, 20, 30, and 40 mN/m.

ods, the dipole potential can be characterized by two parameters, $\mu_\perp$ and ΔV_0. Plots of dipole potential versus concentration for PBPC and its mixtures with SOPC (Fig. 2., *symbols*) exhibited excellent linearity ($R \geq 0.999$, Fig. 2, *solid lines*), as did fits of the other pure phosphatidylcholines (not shown). Theoretical curves for PBPC-containing samples (Fig. 2, *solid lines*) and the values of ΔV_0 and $\mu_\perp$ for the pure lipids obtained from the linear fitting are summarized in Table 1. Values of ΔV_0 for the fluid nonfluorescent lipids average 110 ± 7 mV (Table 1) compared to only 24 mV for PBPC. However, the dipole moment, $\mu_\perp$, of PBPC is 874 mD compared to an average of 495 ± 14 mD for the other lipids, an increase of 77%.

As shown in Figs. 1 and 2 (*symbols*), the surface pressure– and surface potential–concentration isotherms for the PBPC and its mixtures with SOPC exhibit no phase transitions between liftoff and monolayer collapse. The collapse surface pressures for pure lipids and mixtures are shown in Fig. 3 A. The collapse pressures show a slightly sigmoidal variation from the theoretical curve (Fig. 3 A, *solid line*) predicted for ideal miscibility (Joos, 1969). Molecular area-composition plots at selected surface pressures (Fig. 3 B) are, within error, linear at all surface pressures, consistent with ideal miscibility. The miscibility of the lipids can be further characterized using the parameters obtained from

fitting the pressure and potential data as described in Materials and Methods. The variation with mixture composition of A_∞, the fitting parameter representing the hard cylinder area of the lipids, is shown in Fig. 3 C. The parameter shows a continuous change with composition with a slight negative deviation from ideal behavior. The moduli of compression evaluated at 25 mN/m (Fig. 3 D) show almost ideal variation with composition. The behavior of ΔV_0 (Fig. 3 E) shows some deviation from ideality. However, like A_∞, ΔV_0 is obtained by a large mathematical extrapolation of the data. The compositional variation of the dipole moment, $\mu_\perp$, that is determined directly from the slope of the ΔV versus concentration plots, is ideal. Overall, this analysis of surface pressure and dipole potential isotherms establishes the near ideality of PBPC-SOPC mixing in liquid-expanded monolayers. Importantly, it also shows that, despite the presence of the aromatic fluorophore in PBPC, its physical behavior, with the exception of the dipole potential, is similar to that of typical diacylphosphatidylcholines.

Fluorescence of PBPC in SOPC monolayers

Previously, a dimethyl BODIPY-labeled sphingolipid was shown to exhibit concentration-dependent changes in its emission properties consistent with the formation of an excimer species (Pagano et al., 1991). Specifically, with increasing mole fraction of a dimethyl BODIPY-labeled ceramide in small, unilamellar vesicles of 1-palmitoyl-2-oleoyl-*sn*-glycero-3-phosphocholine, the monomer emission at 515 nm was progressively replaced by a broad, featureless excimer emission peak centered at ~620 nm. To characterize the fluorescence behavior of PBPC under more controlled conditions in a planar interface, i.e., mixed monolayers with SOPC, fluorescence emission spectra were obtained as a function of monolayer composition and lipid packing density, i.e., surface pressure. In Fig. 4 spectra obtained with different mole fractions of PBPC in SOPC monolayers at a total lipid concentration of 213 pmol/cm^2 (78 Å^2/molec) are compared. This packing corresponds to a surface pressure of 9.1 mN/m for SOPC and 16.7 mN/m for PBPC (Fig. 1). The spectra are qualitatively similar to those from the earlier bilayer experiment (Pagano et al., 1991). The emission spectra show a peak ($S_0 \rightarrow S_1$) in the vicinity of 520 nm with a shoulder ($S_0 \rightarrow S_2$) at ~540 nm that is characteristic of BODIPY fluorophores (Karolin et al., 1994). At wavelengths >600 nm, a second peak is observed, which has been attributed to the formation of an excimer species.

Absorption spectra of SOPC-PBPC monolayers were also obtained at selected compositions and examples obtained at 0.05, 0.15, and 0.30 mole fraction PBPC and a packing density of 213 pmol/cm^2 are shown in Fig. 5. These essentially mirror the monomer fluorescence peak shown in Fig. 4. The absorption values at the peak maxima in Fig. 5 were proportional to PBPC concentration in the monolayer (not
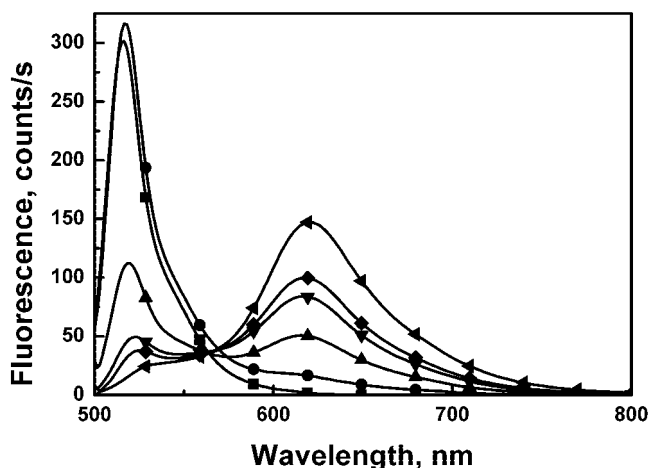
FIGURE 4   Fluorescence emission spectra of PBPC in SOPC monolayers. Spectra were obtained with excitation at 488 nm at a lipid concentration of 213 pmoles/cm^2 for PBPC mole fractions of 0.01 (■); 0.10 (●); 0.20 (▲); 0.40 (▼); 0.50 (◆); 1.00 (◀).

FIGURE 6   Dependence of spectral wavelength maxima on PBPC concentration in SOPC monolayers. Wavelength maxima are shown for PBPC excimer emission (○), monomer emission (●) and absorption (■) measured at a total lipid concentration of 213 pmol/cm^2 (78 Å^2/molec).

shown, $r = 0.995$) and gave an extinction coefficient of 8.0×10^4 cm^{-1}M^{-1}. This agrees reasonably with the value of 8.44×10^4 cm^{-1}M^{-1} at 505 nm determined by us for PBPC in ethanol (Materials and Methods).

Careful inspection of Figs. 4 and 5 shows that the wavelength of the absorption and emission maxima of the dimethyl BODIPY fluorophore increase with PBPC concentration in the monolayers. To characterize the fluorescence behavior of PBPC more extensively, a series of 16 PBPC-SOPC mixtures were prepared with PBPC mole fractions ranging from 0.005 to 1.0. Each mixture was spread as a monolayer on the Kibron trough and compressed to obtain a surface pressure–lipid concentration isotherm of the type shown in Fig. 1. During monolayer compression, monomer and excimer emission intensities, as well as a complete
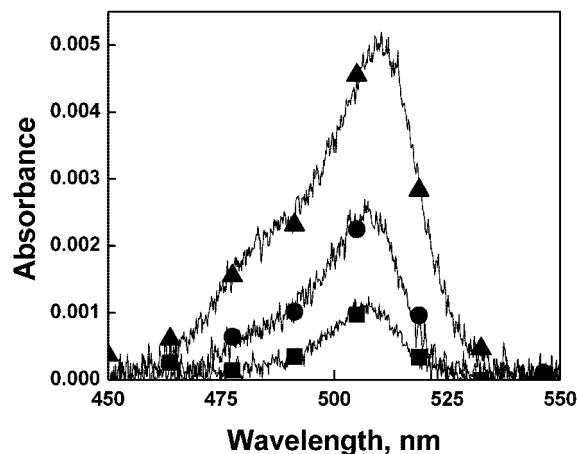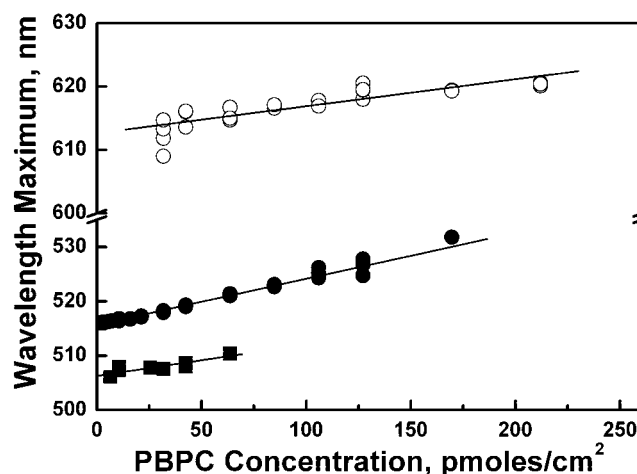

FIGURE 5   Absorbance spectra of PBPC in SOPC monolayers. Spectra were obtained at a total lipid concentration of 213 pmoles/cm^2 (78 Å^2/molec) for PBPC mole fractions of 0.05 (■); 0.15 (●); and 0.30 (▲).

emission spectrum, from the monolayer excited at 488 nm, were recorded every 10 s. Figure 6 shows the wavelength maxima for monomer and excimer emission peaks compared at a total lipid concentration, i.e., PBPC + SOPC, of 213 pmol/cm^2 (78 Å^2/molec). As the concentration of PBPC is increased, there is an approximately linear increase in the emission wavelength maximum of the monomer peak (*filled circles*) from a low value of 515 to a maximum of 535 with a slope of 0.085 nm cm^2/pmol of PBPC. There is a similar shift in the emission maximum wavelength of the excimer (*open circles*) but with a lower slope of 0.043 nm cm^2/pmol of PBPC. Absorption spectra, determined over a smaller range of compositions up to 0.30 PBPC, show a similar shift in the maximum absorption wavelength (*squares*) of 0.057 nm cm^2/pmol. The shift in the absorption wavelength maxima shows that the shift in fluorescence wavelength maxima is mostly due to a change in the ground state properties of the fluorophore as its concentration in the monolayer is increased. Bathochromic shifts in emission maxima are common for dyes that aggregate. If the observed shift is due to PBPC aggregation, however, its linearity over the entire range of concentrations up to nearly pure PBPC suggests that the interaction of the fluorophore with itself must be weak.

Another feature of PBPC fluorescence shown in Fig. 4 is decreased monomer emission intensity as PBPC mole fraction is increased. Such self quenching arises as a consequence of energy transfer among molecules of a fluorophore (van der Meer et al., 1994a) and is also referred to as quenching due to the formation of "statistical traps" (Beddard and Porter, 1976; Boulu et al., 1987; Knoester and Van Himbergen, 1987). Figure 7 (*symbols*) shows a composite of monomer emission intensity–PBPC concentration isotherms obtained for the 16 PBPC mole fractions from 0.005 to 1.00.
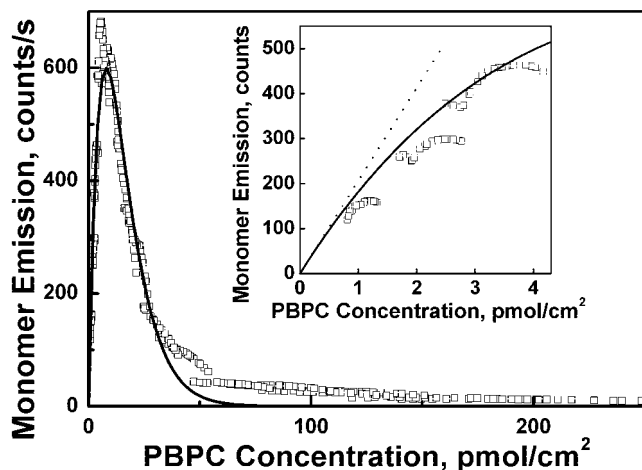
FIGURE 7 Monomer emission of PBPC in SOPC monolayers. Every fifth data point is shown and each point is the average of at least two determinations. Mole fractions of PBPC included are (left to right) 0.005, 0.01, 0.015, 0.025, 0.035, 0.05, 0.075, 0.10, 0.15, 0.20, 0.30, 0.40, 0.50, 0.60, 0.80, and 1.00. The solid line was obtained by fitting the data to Eq. 5 over the entire range of compositions and PBPC concentrations as described in the text. The inset shows data obtained at low mole fractions of PBPC. The dotted line is the expected fluorescence emission in the absence of quenching as determined from the fitting parameters.

At each composition, monomer emission was measured over the range of 1–35 mN/m. The figure shows that, to a reasonable approximation, the 16-monomer emission intensity-concentration isotherms define an essentially continuous curve that rises steeply as the PBPC concentration approaches 10 pmol/cm^2, then falls to essentially zero at higher PBPC concentration, at which the mole fraction of PBPC reaches 1.0 and its interfacial concentration exceeds 200 pmol/cm^2. The approximate continuity of the monomer emission intensity data, that were obtained at different PBPC mole fractions and different surface pressures, shows that self quenching of the dimethyl BODIPY fluorophore depends primarily on the PBPC concentration in the monolayer. Closer inspection of the data sets from Fig. 7 obtained at the three lowest mole fractions of PBPC (Fig. 7, *inset*) shows that, within each set obtained between 1 and 35 mN/m, increasing the PBPC concentration, i.e., surface pressure and total lipid concentration, further enhances quenching. This likely represents the effect of fluorophore orientation on the efficiency of energy transfer (van der Meer et al., 1994b). Although such effects are significant within each data set, they are dwarfed by the overall trend among data sets shown in Fig. 7.

The type of fluorophore concentration dependence of quenching shown in Fig. 7 has been described previously (Boulu et al., 1987) using what is termed a sphere (in this case, circle) of action quenching model (Knoester and Van Himbergen, 1987; Lakowicz, 1999). The basic notion of the model is that emission increases linearly with the two-dimensional concentration of fluorophore, Γ. However, if

two fluorophore molecules are at or within a "critical distance," R_m, they are assumed to form a statistical pair that acts as an exciton trap. In the present case, this can be written in the form,

$$F_m = Q_m \Gamma \exp[-\pi R_m^2 \Gamma], \qquad (5)$$

where the exponential term is the probability of having at least one nearest neighbor at a distance $\leq R_m$. The constant Q_m is a proportionality factor encompassing both the quantum yield of the fluorophore and instrumental parameters. Fitting the data for all 16 mole fractions of PBPC obtained at surface pressures from 1 to 35 mN/m to Eq. 5 gives a correlation coefficient of 0.982. The value for the critical quenching distance is 25.9 ± 1.8 Å and the constant, Q_m, has a value of 206.4 ± 1.3 counts cm^2/pmol s. The theoretical curve is shown as the solid line in Fig. 7 and the initial slope, $Q_m\Gamma$, is shown in the inset as a dotted line. Comparison of these two curves (Fig. 7, *inset*) shows that quenching becomes significant at PBPC concentrations that are realized when the mole fraction of PBPC exceeds 0.005. Using different major subsets of the data, e.g., data from 0 to 0.6 mole fraction, had no effect on the parameters obtained. Because of the monomer spectral shift observed with increasing PBPC concentration (Fig. 6), subsets of data at three fixed total lipid concentrations of 174, 213, and 249 pmol/cm^2 were also analyzed according to the model. This gave essentially identical values of the parameters with $R_m = 25.4–26.7$ Å, showing that the spectral shift does not significantly affect the analysis. The same was true if data at a constant surface pressure of 5 or 30 mN/m were used or if monomer emission intensities at the wavelength maximum for each set were used in place of the average over a range of wavelengths (not shown). Because quenching of the type shown in Fig. 7 can also arise from other than statistical proximity of fluorophore molecules, i.e., specific interaction such as dimerization, the data were also analyzed using a three-parameter form of Eq. 5 (Lakowicz, 1999). This form of the equation incorporates a dissociation constant for fluorophore dimerization in addition to Q_m and R_m. The correlation coefficient was unaltered, and changes to Q_m and R_m were small. Moreover, the value of the apparent dissociation constant was 85 pmol/cm^2. At that concentration, measured monomer emission is quenched >99.9% compared to the value predicted from the dissociation constant, $85Q_m/2$. Thus, probe dimerization does not appear to make a significant contribution to the extensive quenching observed at low PBPC concentrations (Fig. 7).

For each of the 16 monomer emission-intensity–PBPC concentration isotherms shown in Fig. 7, a corresponding excimer emission intensity–PBPC concentration isotherm was also constructed from the fluorescence data measured during compression of each PBPC-SOPC monolayer in the range of 1–35 mN/m. These emission isotherms are shown in Fig. 8 with increasing mole fraction of PBPC from left to
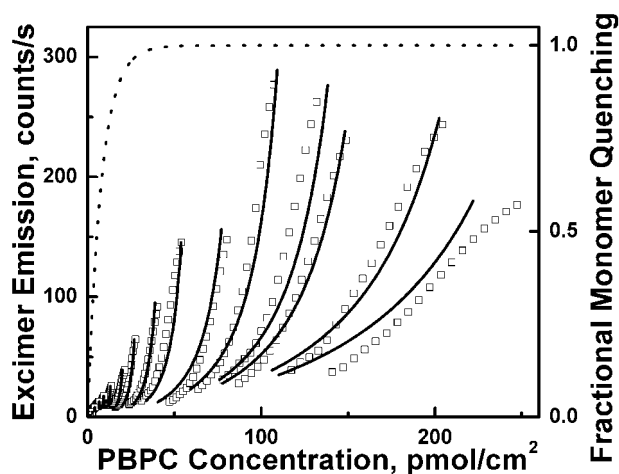
FIGURE 8 Excimer emission of PBPC in SOPC monolayers. Conditions and compositions are as for Fig. 7. The solid lines were obtained by fitting the data to Eq. 6 over the entire range of compositions as described in the text. The dotted line shows the fractional monomer quenching, $1 - F_m/\Gamma Q_m$, predicted using the parameters obtained from fitting the data of Fig. 7.

right. Compared to monomer emission behavior (Fig. 7), excimer emission is markedly different in that the combined isotherms do not define a common curve. Rather, each isotherm obtained at a particular PBPC composition is distinctly displaced from those obtained at higher or lower mole fractions of PBPC. For example, if a vertical line were drawn at the PBPC concentration of 100 pmol/cm^2, it would intersect three isotherms (PBPC mole fractions of 0.4, 0.5, and 0.6 from left to right) at considerably different values of 215, 72, and 45 counts/s. The separation of the isotherms means that, unlike monomer emission, excimer emission is highly sensitive to total lipid concentration (or surface pressure) and to PBPC concentration.

More specifically, Fig. 8 shows that, at any given monolayer composition, excimer emission increases steeply as the lipid monolayer is compressed. At a PBPC mole fraction of 0.5, for example, excimer emission increases by approximately ten-fold over the range of compression, 1–35 mN/m. It is well established that, as fluid monolayers are compressed, the diffusion constant of molecules in the interface decreases three- to ten-fold (Peters and Beck, 1983; Caruso et al., 1993; Tanaka et al., 1999). Thus, the data of Fig. 8 show a qualitatively inverse relation between the rate of lipid translational diffusion and excimer emission intensity at any given PBPC mole fraction. To further test the idea that PBPC excimer emission is inversely related to lipid diffusion, the temperature dependence of the excimer/monomer emission ratio was measured. A monolayer containing 0.15 mole fraction PBPC in SOPC at a surface pressure of 20 mN/m and at constant lipid concentration was cycled from 13°C to 26°C and back to 13°C. During the heating portion of the cycle the ratio decreased from 2.1 to

1.5 and then returned to 2.0 after cooling (data not shown). Most of the changes in the ratio were due to changes in excimer intensity. Qualitatively, the observed temperature dependence of the ratio is opposite what is predicted and observed for the classical diffusion-controlled model of excimer fluorescence in membranes (Galla and Sackmann, 1974). We cannot exclude, however, the possibility that factors other than diffusion determine the temperature dependence of fluorophore emission under the conditions of our experiment.

Diffusion-independent excimer formation can occur from the interaction of a pair of fluorophore monomers that are in close proximity in the ground state (Birks, 1975b). Absorption of a photon by one monomer in proper orientation relative to its neighbor can result in almost instantaneous formation of an excimer. Once formed, such an excimer is indistinguishable from one formed by diffusional collision of an excited monomer and a ground-state monomer. That proximity of dimethyl BODIPY fluorophores is important for excimer formation is suggested by the concentration dependence of excimer fluorescence relative to monomer self quenching. Comparison of the excimer emission (Fig. 8, *symbols*) with the fractional monomer quenching, $(1 - F_m/\Gamma Q_m)$, predicted by the model for monomer emission (Fig. 8, *dotted line*), shows that monomer emission is more than 90% quenched before excimer emission reaches 15% of maximum. This suggests that excimer formation occurs on a length scale, R_e, that is smaller than that for quenching, R_m. Thus, in defining an expression to describe excimer emission in the Appendix, it is assumed that excimer emission is proportional to PBPC concentration, but limited to the statistical fraction of fluorophore molecules that are separated by a distance $\leq R_e$.

If it is assumed that dimethyl BODIPY excimer formation arises from a translational diffusion-independent, proximity-dependent mechanism, how can excimer emission show an apparent inverse correlation with lateral diffusion? This observation suggests that diffusion regulates excimer dissociation, but not by translational diffusion, per se. The rate of lipid translational diffusion is proportional to the molecular jump frequency which, in turn, is proportional to the frequency of *trans-gauche* isomerism, i.e., "kink" formation, in the aliphatic chains of the lipids (Galla et al., 1979). The lifetime of the dimethyl BODIPY probe is in the range of 5–6 ns (Karolin et al., 1994), which is longer than rotational times and kink formation (Galla et al., 1979; König et al., 1992). Thus, these local motions, which ultimately give rise to translational diffusion, can cause excimer dissociation within the lifetime of the excited state. Because $R_e < R_m$, the excited monomer will thermally decay to the ground state. That excimer dissociation/thermal decay is the predominant fate of these excimers is suggested by the observation that excimer emission intensity is maximally only a few hundred counts at high concentrations of PBPC. If excimer quantum yield were comparable to the

calculated value of unquenched monomer emission, $Q_m\Gamma$, at, for example, 100 pmol/cm^2 of PBPC, emission intensity should be 20,600 counts/s.

In deriving a model for excimer emission intensity, it is assumed (Appendix) that emission intensity is inversely proportional to the kink frequency of the chains. Kink frequency is not a readily measurable quantity in fluid monolayers (König et al., 1992). However, as described above, there is a proportional relationship between the kink frequency and the translational diffusion constant of lipids in membranes. Moreover, the diffusion constant can be related to the free area in bilayers (Frijlink et al., 1991; Clegg and Vaz, 1985) or monolayers (Peters and Beck, 1983; Caruso et al., 1993; Tanaka et al., 1999). Thus, as shown in the Appendix, kink frequency and, ultimately, excimer emission intensity can be described in terms of monolayer free area. The impetus for relating kink frequency to free area is that free area can be estimated as the experimentally measurable lipid molecular area at any lipid composition and surface pressure, A, minus the hard cylinder area of the lipid, A_∞. This latter quantity can be calculated from the surface pressure–molecular area isotherm for the lipid mixture as described in Materials and Methods.

Combining the dependencies of excimer fluorescence on PBPC concentration, statistical proximity of PBPC molecules in the monolayer and chain motions as described in the Appendix gives,

$$F_e = Q_e\Gamma[1 - \exp(-\pi R_e^2\Gamma)](A_\infty)^{-1/2}$$
$$\times \exp(\gamma A_\infty/(A - A_\infty)). \qquad (6)$$

The fitting parameters are γ, R_e, and Q_e and represent a correction factor for the overlap of free volumes, the critical distance below which excimers can form and a scaling factor containing the quantum yield, instrumental, and other constants. Analysis of the data shown in Fig. 8 over the entire range of PBPC concentrations and compositions using this model gave a coefficient of correlation of 0.960. The values of Q_e, R_e, and γ are $1.08 \pm 0.03 \times 10^8$ counts cm^3/pmol s, 13.7 ± 3.2 Å, and 1.98. The solid lines show the theoretical fluorescence-concentration isotherm at each PBPC mole fraction calculated using these values of the parameters. The data at the higher mole fractions of PBPC show a tendency to fall off with increasing surface pressure (Fig. 8). This suggests the possibility of some form of higher order excimer formation, as has been described (Birks, 1975a). Because this could affect the values of the parameters, the fitting was repeated using only the data up to 0.60 PBPC. This increased the coefficient of correlation slightly from 0.960 to 0.972 and gave similar values of Q_e, R_e, and γ of $1.56 \pm 0.04 \times 10^8$ counts cm^3/pmol s, 12.0 ± 2.4 Å, and 1.75. Similar changes in the parameters were also observed if the data up to 0.40 or from 0.10 to 1.0 mole fraction of PBPC were used (not shown). This shows that the agreement of the data with the model is fairly robust. Note that, as predicted, R_e is much less than R_m.

Determination of SOPC packing density in unilamellar bilayers

The analysis above shows that both the monomer and excimer emission intensities of PBPC vary continuously with its two-dimensional concentration in lipid monolayers at all PBPC mole fractions. The ratio of the intensities gives a quantity that is independent of measurement variables like absolute intensities, integration times, and optical path. Comparison of this ratio for PBPC in monolayers, where lipid concentration can be continuously varied, and fluid bilayers thus allows the packing density of the lipids in the bilayer to be determined (Thuren et al., 1986). A caveat to the application of this technique, however, is that energy transfer among fluorophores occurs not only in each leaflet of the bilayer, but across the bilayer as well (Loura et al., 2001). To determine the extent to which PBPC in monolayers and bilayers exhibited similar fluorescence behavior, a series of experiments was carried out at differing mole fractions of PBPC ranging from 0.01 to 0.20. A lipid mixture in solvent was prepared for each of eight compositions. Part of that mixture was used to obtain monomer and excimer emission data from monolayers as a function of lipid packing density as described above. Another portion of the mixture was used to prepare 100-nm unilammelar lipid vesicles by extrusion as described in Materials and Methods. The monomer and excimer emission intensities were determined for the bilayer sample using the same spectrofluorimeter used for the monolayer measurements. For each mole fraction of PBPC the excimer/monomer emission ratio of the bilayer sample was compared to those obtained for the monolayer to determine the surface pressure at which they were equal. Using this surface pressure, the apparent molecular area, i.e., the reciprocal of the concentration, of the lipids in the mixture was determined from the ideal surface pressure–area isotherm for the mixture. Ideal isotherms were generated as described in Materials and Methods using data from the surface pressure–concentration isotherms shown in Fig. 1 and the observed nearly ideal miscibility of PBPC and SOPC (Fig. 3 B). Data from Fig. 1 was used for this analysis instead of the measured isotherms because the large trough, automated film balance used to obtain the isotherms of Fig. 1 gives more accurate area values. A plot of the apparent molecular areas obtained as a function of PBPC mole fraction is shown in Fig. 9. The apparent molecular area decreases linearly with decreasing PBPC at a rate of ~6 Å^2 for each 0.10 mole fraction of PBPC in the mixture, reaching a limiting value of 55.6 ± 0.7 Å^2. Because the PBPC concentration is extrapolated to zero, this value represents the molecular area of pure SOPC. Based on the fitted surface pressure–molecular area isotherm for SOPC the monolayer surface pressure equivalent
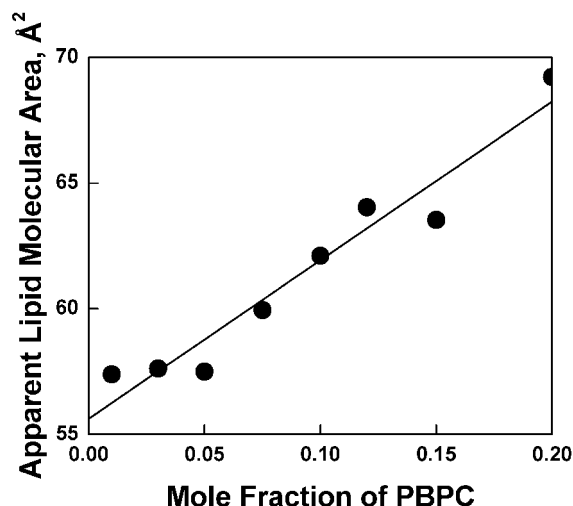
FIGURE 9 Lipid molecular area in unilamellar SOPC vesicles. Molecular area of lipid was obtained by matching the PBPC excimer/monomer emission ratio of vesicles to that of a monolayer with the same PBPC composition to determine the monolayer surface pressure and, hence, molecular area at which the ratio was the same. The solid line is a linear fit of the data.

to the limiting area is 40.5 + 2.1 mN/m, a value ~10% lower than the measured collapse surface pressure of the monolayer.

DISCUSSION

One goal of this work was to determine the extent to which PBPC, with its small rigid fluorophore in the *sn*-2 acyl chain, could be substituted stoichiometrically for typical phosphatidylcholines, like SOPC. Comparison of surface pressure–concentration isotherms of PBPC with other phosphatidylcholines (Fig. 1) showed that PBPC packing density in monolayers is comparable to that of more natural phosphatidylcholines. Although similar in size to other phosphatidylcholines, PBPC has a slightly lower modulus of compression at any surface pressure (Table 1). This is similar to what is observed with 1-stearoyl-2-decanoyl-*sn*-glycero-3-phosphatidylcholine, that also has acyl chains of unequal length (Ali et al., 1998). The dipole potential-concentration isotherm of this chain-mismatched phospholipid is more like that of SOPC. This shows that mismatch, per se, does not give rise to the higher potential values measured for PBPC.

We studied the behavior of PBPC over a wide range of mole fractions with SOPC because the useful photophysical properties of PBPC for monitoring lipid lateral concentration require more than trace quantities of the probe (Chen et al., 1997). Analysis of the data for PBPC-SOPC mixed monolayers showed that mixing is nearly ideal (Fig. 3, *A–D*). This conclusion is supported by dipole-potential measurements (Fig. 3, *E* and *F*). Because the size and shape

of lipid domains in phase-separated systems depends on dipole potential (de Koker and McConnell, 1993), the substitution of PBPC for other phosphatidylcholines could have significant effects on lipid lateral distribution. Otherwise, PBPC behaves physically like more natural phosphatidylcholines. This validates its use as a probe in fluid membranes, even at the relatively high mole fractions observed in some clinical applications (Chen et al., 1999).

One of the major limitations to using the concentration-dependent properties of fluorophores to measure fluorophore concentration in membranes is the tendency of some probes, like pyrenes, to aggregate. Several lines of evidence suggest that this is not a concern for using PBPC in fluid membranes. Part of the evidence, though certainly not conclusive, is the nearly ideal mixing of the probe with SOPC (Fig. 3). Second, the linear shift of monomer emission maximum with increasing PBPC over a 100-fold range of concentrations with no evidence of saturation suggests, at the most, weak interaction between probe molecules. Consistent with this conclusion was the analysis of monomer fluorescence. The data were well described by a simple statistical model ($r = 0.982$), and this was not improved by adding a monomer–dimer quenching equilibrium to incorporate possible probe–probe interaction. Moreover, the value of the quenching dissociation constant obtained using this latter model was so high that, if quenching were solely controlled by such putative dimerization, observed monomer emission intensity at 85 pmol/cm^2 of PBPC should be >8700 counts/s rather than the observed value of ~33. Last, inspection of Fig. 8 shows that, even with a monolayer of PBPC alone, excimer emission intensity increases five-fold between 1 and 35 mN/m, the range of data shown. If PBPC showed a significant tendency to aggregate at lower mole fractions, it should be fully aggregated when every other acyl group contains a BODIPY fluorophore. Why this probe does not show the same tendency to aggregate as planar aromatic fluorophores is suggested by its structure. The planar ring system of dimethyl BODIPY has two fluorine atoms projecting from the plane and two methyl groups that should hinder the close packing of the fluorophore moieties.

What then causes the PBPC concentration-dependent red shift of absorption and emission spectra? One possibility is that substitution of the aromatic fluorophore for hydrocarbon chains increases the dielectric constant of the aliphatic region. This is unlikely, however, because, under dilute conditions, moving BODIPY from an aqueous to a lipidic environment typically shifts spectral peaks by less than 2 nm (Johnson et al., 1991). More likely, the red shift reflects electronic interactions among nonaggregated fluorophores (Birks, 1970) that approach a local bulk concentration of molar in the monolayers.

Self quenching of fluorophores originating from energy transfer involves multiple transfer events. Thus, the efficiency of transfer affects self quenching. For the dimethyl

BODIPY fluorophore, energy transfer is 50% efficient at a distance of $R_0 = 57$ Å (van der Meer et al., 1994a) and should closely approach 99% at ~0.03 mole fraction of PBPC and an average lipid molecular area of 70 Å^2 (Stryer and Haugland, 1967). As a consequence of these factors, quenching in the range of compositions studied is dominated by PBPC concentration, in a manner consistent with a known, simple model (Eq. 5), as shown in Fig. 7. During the compression of a monolayer of a phospholipid like PBPC or SOPC through the liquid-expanded state, total lipid concentration increases approximately two-fold (e.g., Fig. 1, *diamonds/solid line* or *dotted line*). This concentration change is likely accompanied by a change in fluorophore orientation, relative to the monolayer plane, that makes an additional contribution to energy transfer efficiency and, hence, quenching (van der Meer et al., 1994b). Particularly for mixtures at the lowest PBPC concentrations studied, for which simple concentration-dependent quenching is relatively the lowest (Fig. 7 inset, *solid line* versus *dotted line*), changes in fluorophore orientation appear to significantly enhance quenching beyond that predicted solely by PBPC concentration (Fig. 7 inset, *symbols* versus *solid line*). In contrast, at high mole fractions of PBPC, for which PBPC concentration-dependent quenching efficiency alone is predicted to be >99.9% (e.g., Fig. 7, *solid line* at ~100 pmol/cm^2 of PBPC), the addition of an orientational quenching contribution has a smaller effect on measured monomer emission.

Excimer emission by PBPC appears to be highly inefficient. This can be explained by the apparent lack of fluorophore aggregation, the short excited-state lifetime relative to lipid translational diffusion, the requirement for fluorophore proximity for excimer formation (but not necessarily emission) and a need for relatively high total lipid packing density to counteract excimer dissociation and to ensure proper fluorophore orientation (Fig. 8). The data over a wide range of PBPC concentrations and total lipid packing densities are well described by the proposed model (Eq. 6). The parameter γ in Eq. 6 is a correction factor for the overlap of free areas and can have values from 0.5 to 1.0 (Galla et al., 1979; Clegg and Vaz, 1985). The value of 1.98 obtained is twice theoretical for reasons not presently understood. The fitted critical distance for excimer emission, $R_e = 13.7$ Å, is approximately one-half of that for quenching, $R_m = 25.9$ Å, which, in turn, is about one-half of $R_0 = 57$ Å. The significance of these particular relationships, if any, is not apparent, other than that the parameters fall in the expected order of $R_e < R_m < R_0$, and that the value of R_m is the distance at which the calculated energy transfer efficiency exceeds 99%. Thus, excimers form predominantly under conditions where monomer emission is almost completely quenched. This helps to explain why organelles in cells labeled with dimethyl BODIPY-containing lipids appear visually green (monomer) or red-orange (excimer) (Chen et al., 1997).

Even though the physical characteristics of PBPC show it to be a reasonable substitute for typical phosphatidylcholines in membranes at all compositions, its usefulness as a fluorophore to quantitate lateral lipid concentration or composition is practically limited to a range of compositions. This is a consequence of the separation of the two modes of PBPC emission with respect to their dependence on PBPC concentration (Figs. 7 and 8) and because methods based on the ratio of fluorescence quantities are less prone to systematic errors than those that rely on absolute intensities. PBPC monomer emission intensity is so highly quenched that, above 0.20 mole fraction, the monomer peak is small. In contrast, excimer emission is so dependent on fluorophore proximity that it becomes difficult to measure below 0.01 mole fraction. Thus, the most useful range for using the PBPC excimer/monomer emission ratio to assess lipid packing density appears to be 0.01–0.20 mole fraction.

The analysis presented in this work shows that both the monomer and excimer fluorescence emission intensities of PBPC depend linearly on its mole fraction in a membrane. However, excimer emission intensity depends much more strongly on total lipid concentration than does monomer emission intensity. These properties of PBPC emission show that the implicit assumption that the emission properties of dimethyl BODIPY-labeled lipids in cells are the same as those in phospholipid bilayer vesicles (Pagano et al., 1999) is only approximately correct. To what extent differences in lipid packing density between natural membranes and the model phosphatidylcholine membranes used for calibration practically affects results cannot presently be assessed. This is largely because it is difficult or impossible to measure lipid packing density in either model or natural fluid bilayer membranes (Costigan et al., 2000).

Attempts have been made to determine packing density in unilamellar bilayers by equilibrating lipid monolayers and excess unilamellar bilayers in the aqueous subphase. However, results have been conflicting because of the need for long equilibration times, sensitivity to impurities, and bilayer hemifusion to monolayers. Using an improved version of the technique, it was shown recently that the monolayer surface pressure generated by a variety of bilayers was ~47 mN/m (Lee et al., 2001), a value typical for the measured collapse pressure of phospholipid monolayers (Table 1). This value was independent of differences in lipid packing density that were inferred from differences in acyl chain unsaturation and independent of the presence of cholesterol. The value is, however, similar to the energy of a simple hydrocarbon–water interface. This suggested to the authors that the collapse of phospholipid monolayers may be driven by the hydrocarbon chains alone and implies that the lipid packing density of a monolayer at collapse may not equal that of the bilayer from which it was formed. Estimates obtained by techniques other than direct monolayer–bilayer equilibration, e.g., susceptibil-

ity to enzymatic degradation, place bilayer membrane packing densities equivalent to those of monolayers in the range of 30–35 mN/m (MacDonald, 1996; Marsh, 1996). To determine lipid packing density in unilamellar lipid bilayers of SOPC, we used the fluorescence behavior of PBPC in monolayers and bilayers as described in Results. The molecular area of SOPC in unilamellar bilayers was found to be 55.6 ± 0.7 Å^2 (299 pmol/cm^2), which is equivalent to a monolayer surface pressure of 40.5 ± 2.1 mN/m. The molecular area is lower than the value of 61.4 Å^2 determined from multilamellar bilayers at 30°C (Koenig et al., 1997). Factors possibly responsible for the difference in reported values are the difference in temperature, the lamellarity of the bilayers and differences in ionic strength.

Overall, the results presented show that PBPC is a reasonable substitute for physiologically-relevant phosphatidylcholines commonly used in membrane research and that its fluorescence properties are simple, relative to pyrenes (Lemmetyinen et al., 1989), in that excimer formation arises predominantly by a single mechanism. The analysis of PBPC fluorescence provides a theoretical basis for using the fluorescence of this and related lipids, as demonstrated, to determine lateral lipid concentrations and, potentially, their perturbation by membrane-active substances. The need for close fluorophore proximity for excimer emission should be useful in near-field optical microscopy to quantitate the lateral distribution of lipids in the vicinity of proteins and other structures in membranes (Hwang et al., 1995). Preliminary studies from this laboratory have already shown that the local concentration of BODIPY-labeled lipids in the vicinity of colipase depends on the species in which the BODIPY group resides.

APPENDIX

Based on the observations presented and data in the literature, we assume the following properties of excimer fluorescence intensity, F_e:

1. $F_e \propto \Gamma$; where Γ is the two-dimensional concentration of PBPC.
2. Whereas only fluorophore molecules separated by more than a distance, R_m, can emit monomer fluorescence, only molecules that are separated by less than a critical distance, R_e, can form excimers. It is assumed, but not required, that $R_e < R_m$. By analogy to the critical distance model for the quenching of monomer fluorescence,

$$F_e \propto [1 - \exp(-\pi R_e^2 \Gamma)].$$

3. Excimer formation by molecules separated by $<R_e$ is essentially instantaneous.
4. Excimer emission is inefficient relative to its dissociation.
5. The probability of excimer dissociation is proportional to the *trans–gauche* kink frequency of the acyl chains, ν_k.

Therefore,

$$F_e \propto 1/\nu_k.$$

However, kink diffusion is the origin of lateral diffusion and ν_k is related to the lateral jump frequency, ν_j, by

$$\nu_k = (L^2/2d_k^2)\nu_j,$$

where L is the length of the diffusing molecule and d_k is the lateral displacement of the chain caused by *trans–gauche* isomerism (Galla and Sackmann, 1974). These parameters are assumed to be constant. The jump frequency is related to the lateral diffusion coefficient, D, by the relation

$$D = \nu_j \lambda^2/4,$$

where λ is the average diffusional jump length and is assumed to be constant (Galla et al., 1979). The diffusion coefficient can also be expressed as

$$D = gl_c\mu \exp(-\gamma a^*/a_f),$$

where g is a constant with a value in two dimensions of ¼, μ is the kinetic velocity of a lipid molecule, and γ is a factor between 0.5 and 1.0, which corrects for overlap of free volumes (Galla et al., 1979; Clegg and Vaz, 1985). For a given fluorophore at a fixed temperature, μ is a constant. The parameter a^* is the critical area necessary for a jump to occur and has been equated with the hard cylinder or van der Waals area of the molecule. The parameter l_c is defined as the average length of travel within the free area and is roughly the diameter of the cage with area a^*. Combining relationships to eliminate D and ν_j gives

$$\nu_k = [2L^2g\mu/d_k^2\lambda^2]l_c\exp(-\gamma a^*/a_f),$$

which describes the kink frequency, ν_k, as a function of constants and the variables l_c, a^*, and a_f. The free area model of diffusion on which this derivation is based was adapted from the three-dimensional form (Cohen and Turnbull, 1959) to describe diffusion in two dimensions (Galla et al., 1979; Clegg and Vaz, 1985) and is supported by neutron diffraction measurements (König et al., 1992).

As described in Materials and Methods, monolayer surface pressure–molecular area isotherms for both single and multi-component mixed monolayers can be fitted to obtain the molecular area at infinite surface pressure, A_∞. We equate this area with a^* and, hence, from above,

$$l_c = 2(\sqrt{A_\infty/\pi}) \quad \text{and} \quad a_f = (A - A_\infty).$$

Making these substitutions into the expression for ν_k and combining with the proportionalities described in properties 1 and 2 above gives,

$$F_e = Q_e\Gamma[1 - \exp(-\pi R_e^2\Gamma)](A_\infty)^{-1/2}$$
$$\times \exp(\gamma A_\infty/(A - A_\infty)),$$

where Q_e combines all constant terms, including the quantum efficiency of the probe and instrumental parameters. It should be noted that, whereas Γ is the two-dimensional concentration of the fluorescent lipid, A is the reciprocal of the total lipid concentration. Both terms are known from the monolayer experiment.

REFERENCES

Ali, S., J. M. Smaby, H. L. Brockman, and R. E. Brown. 1994. Cholesterol's interfacial interaction with galactosylceramides. *Biochemistry* 33:2900–2906.

Ali, S., J. M. Smaby, M. M. Momsen, H. L. Brockman, and R. E. Brown. 1998. Acyl chain-length asymmetry alters the interfacial elastic interactions of phosphatidylcholines. *Biophys. J.* 74:338–348.

Bartlett, G. R. 1959. Phosphorus assay in column chromatography. *J. Biol. Chem.* 234:466–469.

Baumann, J., and M. D. Fayer. 1986. Excitation transfer in disordered two-dimensional and anisotropic three-dimensional systems: effects of spatial geometry on time-resolved observables. *J. Chem. Phys.* 85: 4087–4107.

Beddard, G. S., and G. Porter. 1976. Concentration quenching in chlorophyll. *Nature.* 260:366–367.

Bergström, F., P. Hägglöf, J. Karolin, T. Ny, and L. B. Å. Johansson. 1999. The use of site-directed fluorophore labeling and donor–donor energy migration to investigate solution structure and dynamics in proteins. *Proc. Natl. Acad. Sci. U.S.A.* 96:12477–12481.

Birks, J. B. 1970. Photophysical processes. *In* Photophysics of Aromatic Molecules. J. B. Birks, editor. Wiley-Interscience, London. 29–43.

Birks, J. B. 1975a. Excimers. *Rep. Prog. Phys.* 38:903–974.

Birks, J. B. 1975b. The photophysics of aromatic excimers. *In* The Exciplex. M. Gordon and W.R. Ware, editors. Academic Press Inc., New York. 39–73.

Boulu, L. G., L. K. Patterson, J. P. Chauvet, and J. J. Kozak. 1987. Theoretical investigation of fluorescence concentration quenching in two-dimensional disordered systems. Application to chlorophyll *a* in monolayers of dioleylphosphatidylcholine. *J. Chem. Phys.* 86:503–507.

Brockman, H. L. 1994. Dipole potential of lipid membranes. *Chem. Phys. Lipids.* 73:57–79.

Brockman, H. L., C. M. Jones, C. J. Schwebke, J. M. Smaby, and D. E. Jarvis. 1980. Application of a microcomputer controlled film balance system to collection and analysis of data from mixed monolayers. *J. Colloid Interface Sci.* 78:502–512.

Caruso, F., F. Grieser, P. J. Thistlethwaite, and M. Almgren. 1993. Two-dimensional diffusion of amphiphiles in phospholipid monolayers at the air–water interface. *Biophys. J.* 65:2493–2503.

Chen, C.-S., O. C. Martin, and R. E. Pagano. 1997. Changes in the spectral properties of a plasma membrane lipid analog during the first seconds of endocytosis in living cells. *Biophys. J.* 72:37–50.

Chen, C.-S., M. C. Patterson, C. L. Wheatley, J. F. O'Brien, and R. E. Pagano. 1999. Broad screening test for sphingolipid-storage diseases. *Lancet.* 354:901–905.

Clegg, R. M., and W. L. C. Vaz. 1985. Translational diffusion of proteins and lipids in artificial lipid bilayer membranes. A comparison of experiment with theory. *In* Progress in Protein–Lipid Interactions. A. Watts and J. J. H. H. M. De Pont, editors. Elsevier Science Publishers B.V., Amsterdam, The Netherlands. 173–229.

Cohen, M. H., and D. Turnbull. 1959. Molecular transport in liquids and glasses. *J. Chem. Phys.* 31:1164–1169.

Costigan, S. C., P. J. Booth, and R. H. Templer. 2000. Estimations of lipid bilayer geometry in fluid lamellar phases. *Biochim. Biophys. Acta.* 1468:41–54.

de Koker, R., and H. M. McConnell. 1993. Circle to dogbone: shapes and shape transitions of lipid monolayer domains. *J. Phys. Chem.* 97: 13419–13424.

Farber, S. A., M. Pack, S.-Y. Ho, I. D. Johnson, D. S. Wagner, R. Dosch, M. C. Mullins, H. S. Hendrickson, E. K. Hendrickson, and M. E. Halpern. 2001. Genetic analysis of digestive physiology using fluorescent phospholipid reporters. *Science.* 292:1385–1388.

Feng, S., H. L. Brockman, and R. C. MacDonald. 1994. On osmotic-type equations of state for liquid-expanded monolayers of lipids at the air–water interface. *Langmuir.* 10:3188–3194.

Frijlink, H. W., A. C. Eissens, N. R. Hefting, K. Poelstra, C. F. Lerk, and D. K. F. Meijer. 1991. The effect of parenterally administered cyclodextrins on cholesterol levels in the rat. *Pharm. Res.* 8:9–16.

Gaines, G. L., Jr. 1966. Mixed monolayers. *In* Insoluble Monolayers at Liquid–Gas Interfaces. I. Prigogine, editor. Interscience Publishers/John Wiley and Sons, New York. 281–300.

Galla, H.-J., W. Hartmann, U. Theilen, and E. Sackmann. 1979. On two-dimensional passive random walk in lipid bilayers and fluid pathways in biomembranes. *J. Membr. Biol.* 48:215–236.

Galla, H.-J., and E. Sackmann. 1974. Lateral diffusion in the hydrophobic region of membranes: use of pyrene excimers as optical probes. *Biochim. Biophys. Acta.* 339:103–115.

Hwang, J., L. K. Tamm, C. Böhm, T. S. Ramalingam, E. Betzig, and M. Edidin. 1995. Nanoscale complexity of phospholipid monolayers investigated by near-field scanning optical microscopy. *Science.* 270: 610–614.

Johnson, I. D., H. C. Kang, and R. P. Haugland. 1991. Fluorescent membrane probes incorporating dipyrrometheneboron difluoride fluorophores. *Anal. Biochem.* 198:228–237.

Joos, P. 1969. Theory on the collapse pressure of mixed insoluble monolayers with miscible components. *Bull. Soc. Chim. Belg.* 78:207–217.

Kaiser, R. D., and E. London. 1998. Determination of the depth of BODIPY probes in model membranes by parallax analysis of fluorescence quenching. *Biochim. Biophys. Acta.* 1375:13–22.

Karolin, J., L. B. Å. Johansson, L. Strandberg, and T. Ny. 1994. Fluorescence and absorption spectroscopic properties of dipyrrometheneboron difluoride (BODIPY) derivatives in liquids, lipid membranes, and proteins. *J. Am. Chem. Soc.* 116:7801–7806.

Kasurinen, J. 1992. A novel fluorescent fatty acid, 5-methyl-BDY-3-dodecanoic acid, is a potential probe in lipid transport studies by incorporating selectively to lipid classes of BHK cells. *Biochem. Biophys. Res. Commun.* 187:1594–1601.

Knoester, J., and J. E. Van Himbergen. 1987. On the theory of concentration self-quenching by statistical traps. *J. Chem. Phys.* 86:3571–3576.

Koenig, B. W., H. H. Strey, and K. Gawrisch. 1997. Membrane lateral compressibility determined by NMR and x-ray diffraction: effect of acyl chain polyunsaturation. *Biophys. J.* 73:1954–1966.

König, S., W. Pfeiffer, T. Bayerl, D. Richter, and E. Sackmann. 1992. Molecular dynamics of lipid bilayers studied by incoherent quasi-elastic neutron scattering. *J. Phys. (Paris).* 2:1589–1615.

Ladokhin, A. S., S. Jayasinghe, and S. H. White. 2000. How to measure and analyze tryptophan fluorescence in membranes properly, and why bother? *Anal. Biochem.* 285:235–245.

Lakowicz, J. R. 1999. Quenching of fluorescence. *In* Principles of Fluorescence Spectroscopy. Kluwer Academic/Plenum Publishers, New York. 237–265.

Lee, S., D. H. Kim, and D. Needham. 2001. Equilibrium and dynamic interfacial tension measurements at microscopic interfaces using a micropipet technique. 2. Dynamics of phospholipid monolayer formation and equilibrium tensions at the water–air interface. *Langmuir.* 17: 5544–5550.

Lemmetyinen, H., M. Yliperttula, J. Mikkola, J. A. Virtanen, and P. K. J. Kinnunen. 1989. Kinetic study of monomer and excimer fluorescence of pyrene-substituted phosphatidylcholine in phosphatidylcholine bilayers. *J. Phys. Chem.* 93:7170–7175.

Lentz, B. R., and S. W. Burgess. 1989. A dimerization model for the concentration dependent photophysical properties of diphenylhexatriene and its phospholipid derivatives DPHpPC and DPHpPA. *Biophys. J.* 56:723–733.

Li, X.-M., M. M. Momsen, J. M. Smaby, H. L. Brockman, and R. E. Brown. 2001. Cholesterol decreases the interfacial elasticity and detergent solubility of sphingomyelins. *Biochemistry.* 40:5954–5963.

Loura, L. M. S., R. F. M. de Almeida, and M. Prieto. 2001. Detection and characterization of membrane microheterogeneity by resonance energy transfer. *J. Fluoresc.* 11:197–209.

MacDonald, R. C. 1996. The relationship and interactions between lipid bilayers vesicles and lipid monolayers at the air/water interface. *In* Vesicles. M. Rosoff, editor. Marcel Dekker, New York. 3–48.

MacDonald, R. C., R. I. MacDonald, B. P. M. Menco, K. Takeshita, N. K. Subbarao, and L. Hu. 1991. Small-volume extrusion apparatus for prep-

aration of large, unilammellar vesicles. *Biochim. Biophys. Acta.* 1061: 297–303.

Marsh, D. 1996. Lateral pressure in membranes. *Biochim. Biophys. Acta.* 1286:183–223.

Merkel, R., and E. Sackmann. 1994. Nonstationary dynamics of excimer formation in two-dimensional fluids. *J. Phys. Chem.* 98:4428–4442.

Momsen, M. M., M. Dahim, and H. L. Brockman. 1997. Lateral packing of the pancreatic lipase cofactor, colipase, with phosphatidylcholine and substrates. *Biochemistry.* 36:10073–10081.

Pagano, R. E., O. C. Martin, H. C. Kang, and R. P. Haugland. 1991. A novel fluorescent ceramide analogue for studying membrane traffic in animal cells: accumulation at the Golgi apparatus results in altered spectral properties of the sphingolipid precursor. *J. Cell Biol.* 113: 1267–1279.

Pagano, R. E., R. Watanabe, C. Wheatley, and C.-S. Chen. 1999. Use of *N*-[5-(5,7-dimethyl boron dipyrromethene difluoride-sphingomyelin to study membrane traffic along the endocytic pathway. *Chem. Phys. Lipids.* 102:55–63.

Peters, R., and K. Beck. 1983. Translational diffusion in phospholipid monolayers measured by fluorescence microphotolysis. *Proc. Natl. Acad. Sci. U.S.A.* 80:7183–7187.

Rodriguez, F., J.-F. Tocanne, and A. Lopez. 1995. Self-association processes involving anthracene labeled phosphatidylcholines in model membrane. *Biophys. Chem.* 53:169–180.

Smaby, J. M., and H. L. Brockman. 1990. Surface dipole moments of lipids at the argon–water interface. Similarities among glycerol-ester-based lipids. *Biophys. J.* 58:195–204.

Smaby, J. M., and H. L. Brockman. 1991. An evaluation of models for surface pressure–area behavior of liquid-expanded monolayers. *Langmuir.* 7:1031–1034.

Smaby, J. M., and H. L. Brockman. 1992. Characterization of lipid miscibility in liquid-expanded monolayers at the gas–liquid interface. *Langmuir.* 8:563–570.

Stryer, L., and R. P. Haugland. 1967. Energy transfer: a spectroscopic ruler. *Proc. Natl. Acad. Sci. U.S.A.* 58:719–726.

Tanaka, K., P. A. Manning, V. K. Lau, and H. Yu. 1999. Lipid lateral diffusion in dilauroylphosphatidylcholine/cholesterol mixed monolayers at the air/water interface. *Langmuir.* 15:600–606.

Thuren, T., J. A. Virtanen, and P. K. J. Kinnunen. 1986. Estimation of the equilibrium lateral pressure in 1-palmitoyl-2-[6(pyren-1-yl)]-hexanoyl-glycerophopholipid liposomes. *Chem. Phys. Lipids.* 41:329–334.

van der Meer, B. W., G. Coker, III, and S.-Y. S. Chen. 1994a. Concepts. *In* Resonance Energy Transfer. Theory and Data. VCH Publishers, New York.5–33.

van der Meer, B. W., G. Coker, I. I. I., and S.-Y. S. Chen. 1994b. Kappa Squared. *In* Resonance Energy Transfer. Theory and Data. VCH Publishers, Inc., New York. 55–83.

Wories, H. J., J. H. Koek, G. Lodder, J. Lugtenburg, R. Fokkens, O. Driessen, and G. R. Mohn. 1985. A novel water-soluble fluorescent probe: synthesis, luminescence and biological properties of the sodium salt of the 4-sulfonato-3,3′,5,5′-tetramethyl-2,2′-pyrromethen-1,1′-BF$_2$ complex. *Recl. Trav. Chim. Pays-Bas.* 104:288–291.